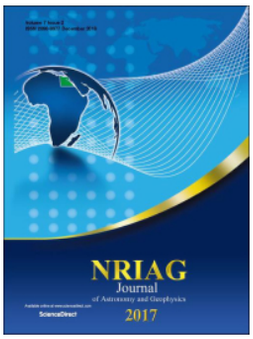

NRIAG Journal of Astronomy and Geophysics

ISSN: (Print) (Online) Journal homepage: https://www.tandfonline.com/loi/tjag20

The influence of flight height and overlap on UAV imagery over featureless surfaces and constructing formulas predicting the geometrical accuracy

Ahmed Elhadary, Mostafa Rabah, Essam Ghanim, Rasha Mohie & Ahmed Taha

To cite this article: Ahmed Elhadary, Mostafa Rabah, Essam Ghanim, Rasha Mohie & Ahmed Taha (2022) The influence of flight height and overlap on UAV imagery over featureless surfaces and constructing formulas predicting the geometrical accuracy, NRIAG Journal of Astronomy and Geophysics, 11:1, 210-223, DOI: 10.1080/20909977.2022.2057148

To link to this article: https://doi.org/10.1080/20909977.2022.2057148

Published online: 04 Apr 2022.

NRIAG JOURNAL OF ASTRONOMY AND GEOPHYSICS
2022, VOL. 11, NO. 1, 210–223
https://doi.org/10.1080/20909977.2022.2057148

The influence of flight height and overlap on UAV imagery over featureless surfaces and constructing formulas predicting the geometrical accuracy

Ahmed Elhadary, Mostafa Rabah, Essam Ghanim, Rasha Mohie and Ahmed Taha

Department of Civil Engineering, Benha Faculty of Engineering, Benha University, Benha, Egypt

ABSTRACT

The improvement of unmanned aerial system and photogrammetric computer vision (CV) algorithms has presented an aerial imaging technique for high accuracy and low-cost alternatives for mapping and topographic applications. Structure from motion (SFM) is an automation photogrammetric CV algorithm used for generating 3D coloured point clouds and 3D models from overlapping images. One of the biggest problems preventing the automation extraction and matching key points in the aligning aerial images is the non-texture of the covered area surface. This paper assessed the effect of flight altitude and overlap degree on 3D point clouds' geometric accuracy and models produced by unmanned aerial vehicle (UAV) images captured over non-textured sandy areas. Four flight altitudes (140, 160, 180 and 200 m) related to spatial resolution (3.41, 3.9, 4.39 and 4.68 cm/pix ground sample distance (GSD)), respectively, and three overlap levels (60%, 70% and 80%) were assessed using RGB images captured by UX5 UAV over a non-textured sandy area in Jahra, Kuwait. The results showed that altitude increment might reduce flight time, processing time and cost, keeping with the acceptable and suitable geometric accuracy. Generally, favourable results are obtained for the four altitudes and overlap degrees of 80% at least. Multivariate nonlinear regression analysis was used to fit the relation between geometric accuracy, image overlap and GSD cm/pixel for the seven missions determining two formulas that predict the geometrical accuracy of the UAV point cloud with a precision of 92.76% and 91.91% for both formulas.

ARTICLE HISTORY
Received 25 January 2022
Revised 9 March 2022
Accepted 18 March 2022

KEYWORDS
UAV flight configuration; flight altitude effect; overlap degree; non-textured surface

1. Introduction

Unlike conventional topographic survey techniques and satellite imagery, images captured by unmanned aerial vehicle (UAVs) have advantages of low platform cost, flexibility, rapid, high resolution and precise positioning and no need for permissions in most countries. Based on these advantages, photogrammetry based on the UAV platform has become a popular technique in mapping topographic applications. Capturing imagery by a camera installed in UAV has importance in cartographic (Crommelinck et al. 2017), remote sensing (Aasen et al. 2018), agriculture (Borgogno Mondino and Gajetti 2017), environmental (Manfreda et al. 2018) and metrology (Daakir et al. 2017) applications.

Using UAVs as a photogrammetric platform have the ability to overfly and capture wide accessible or inaccessible or dangerous areas within a short time with high resolution due to the low altitude of flying. For the geomatics applications, a geo-referencing of the captured images is required to determine the points' 3D location in a certain reference system. There are two methods of determining the exterior orientation (EO) parameters for each image in aerial imaging. The first way is integrating the measurements from the differential global navigational satellite system (DGNSS) and the inertial measurement system. This technique is called direct geo-referencing (DG). The second way is the indirect geo-referencing (IG), which uses the good distribution of ground control points (GCPs) to compute the EO parameters (Rabah et al. 2018).

In addition to the processing parameters, UAV photogrammetry output products' accuracy is affected by the field configuration like flight height, which determines the pixel size of the images and defines the spatial quality, overlap and side lap and distribution of GCPs (Mesas-Carrascosa et al. 2016). There are some problems that affect the automatic matching and the efficiency of image processing. One of the biggest problems is the featureless surface, which prevents and affects the scale-invariant feature transform (SIFT) process. To overcome this problem, flight field configuration parameters must be taken into consideration before flight data acquisition.

The UAV altitude above ground lLevel (AGL) and degree of image overlap affect the accuracy and efficiency of aligning and automatic matching step in the SIFT process. The image overlap offers enough corresponding points in sequence images to match and

CONTACT Ahmed Elhadary ahmedelhadary1992@yahoo.com; ahmed.elhadari@bhit.bu.edu.eg Department of Civil Engineering, Benha Faculty of Engineering, Benha University, Egypt

align them. The overlap degree should be enough or the photos cannot be aligned. The effect of overlap is divided into two portions: the forward and the side overlap. The number of photos per second manages the forward overlap, and the side overlap is managed in the flight planning (Falkner and Morgan 2002).

$$o_{forward} = \left(1 - \frac{d_{forward} * f}{H * W}\right) * 100$$

$$o_{side} = \left(1 - \frac{d_{side} * f}{H * W}\right) * 100$$

Where

$o_{forward}$: The forward overlap %, o_{side}: The side overlap %.

$d_{forward}$: The distance between two sequence image centres (m).

d_{side}: The distance between two successive flight lines (m).

f: The camera focal length (mm), W: The sensor width (mm).

H: The height of the camera above the ground (m).

GSD or spatial resolution is calculated by $GSD = \frac{p}{f}H$, where p is the pixel size on the sensor and GSD is the distance between two sequence pixel centres measured on the ground.

Domingo et al. (2019) assessed the influence of image resolution, camera type and side overlap on models constructed from UAV data. The results showed that the accuracy increased when using finer image resolution and RGB camera. Seifert et al. (2019) studied the effects of drone flight parameters on image reconstruction and successful 3D point extraction. Low flight altitudes yielded the highest reconstruction details and best precisions. Çelik et al. (2020) investigated the effect of flight height on DSM and orthophoto. Compared to a flight height of 50 m, a more detailed and high-resolution model was created with 30 m. As a result of this comparison, it was determined that the flight height should be determined according to the terrain structure, accuracy, precision and time–cost balance expected from the job. From previous researches, although the featureless surface of the covered area surface is one of the biggest problems and obstacles of image processing, no articles discuss and study this parameter.

This paper aims to study the effect of flight altitude AGL and image overlap degree on point extraction, matching, image reconstruction and the geometric accuracy of 3D point clouds and models generated by UAV images over featureless flat areas. For understanding the influence of UAV variables on the precision of reconstruction detail and image matching parameters during IG and DG processing, this study explored seven different flights:

(1) Four different flight height AGL (140, 160, 180 and 200 m) with image spatial resolution (3.41, 3.9, 4.39 and 4.68 cm/pix GSD), respectively.
(2) Three levels of the image forward and lateral overlap (60 %, 70 %, and 80 %) using 160 m flight altitude.

The other purpose is forming mathematical formulas to predict the UAV point cloud's geometrical accuracy by changing the GSD cm/pix and image overlap ratio.

2. Research methodology

2.1. The study area

The seven different altitudes AGL and overlap degree missions were performed on the part of a desert located in Jahra, Kuwait (centred at latitude = 29° 13' 4.54"N' and longitude = 47° 39' 45.14" E). Figure 1 shows the test area on Google maps.

2.2. Photogrammetric data acquisition

The seven photogrammetric data acquisition has been performed of four different height AGL and three different overlap degrees with image format 6000 × 4000 pixels using 16 mm focal length SONY ILCE-5100 camera equipped with a fixed-wing UAV UX5 vehicle with 1 m wing length. Figure 2 shows the

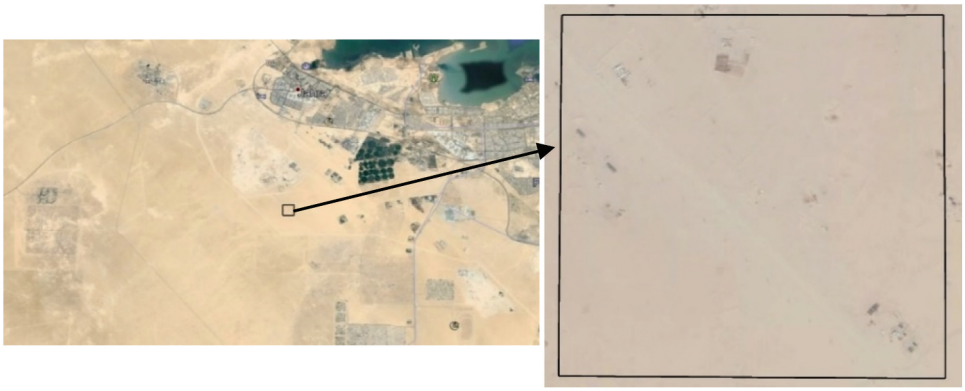

Figure 1. The test area on Google maps.

Figure 2. The used UX5 UAV and SONY camera.

Figure 3. Sample of the acquired UAV images.

used UAV and camera, and Figure 3 shows a sample of the acquired images. The ground points are needed for geo-referencing the photogrammetric output products. Thirteen ground targets were set up, consisting of black–white square plates determined by static GNSS; Figure 4 shows the identification of the ground points. Five points used as GCPs were chosen in each corner and centre, and the remaining eight points were used as independent checkpoints (ICPs); Figure 5 shows the locations of the GCPS and ICPs.

Seven flights were planned to test the influence of the altitude AGL and image overlap degree in the accuracy of processing UAV images covering featureless flat areas, as presented in Figure 6. These seven flights include four different altitudes of 140, 160, 180 and 200 m AGL and three different overlaps of 60%, 70% and 80%. Each altitude is connected to GSD ranging from 3.41 cm/pixel at 140 m to 4.68 cm/pixel at 200 m. The seven data acquisition is processed by the two techniques IG and DG by five GCPs

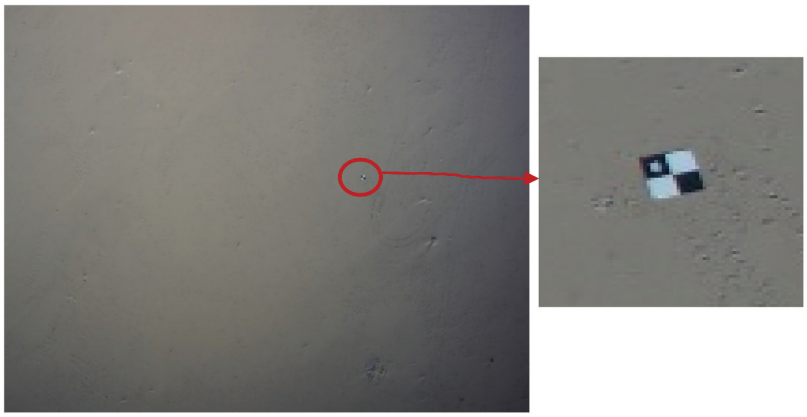

Figure 4. The identification of GCPs in images.

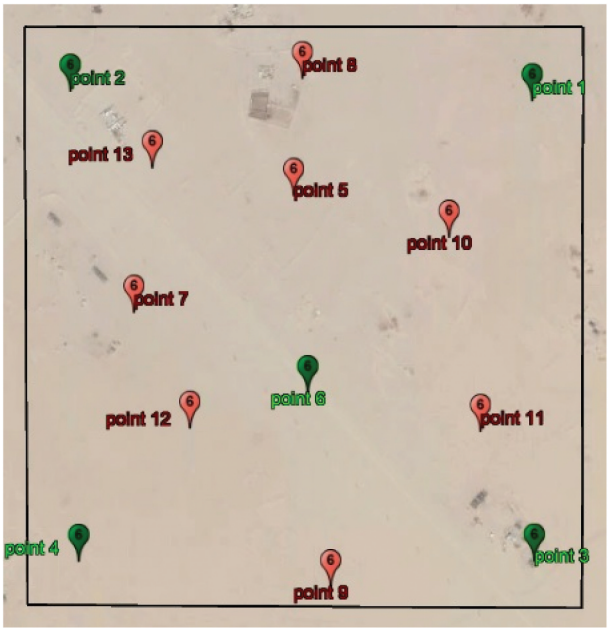

Figure 5. The locations of 5 GCPs (green mark) and 8 ICPs (red mark).

determined by static GNSS and EO parameter determined by RTK-GNSS and eight ICPs used as checkpoints. All the flight missions were performed under the same parameters and wind conditions; thus, the accuracy of generated products is only dependent on flight altitude or overlap degree.

2.3. Photogrammetric data processing

After the photogrammetric missions are performed, the obtained UAV images are processed through Agisoft Metashape professional 1.6.0 software. The processing provides 3D coloured point clouds and 3D photogrammetric models of the study area. The process is performed in two main steps. First, aligning and matching the images. Second, geo-referencing the images, as shown in Figure 7 (Agisoft 2019).

3. Results and discussions

Seven different missions, four different altitude AGL and three different image overlap degrees as shown in Figure 6 were tested and analysed to show the effect of field configuration on the spatial accuracy of the generated point clouds by UAV featureless images. Thirteen ground points were measured by static GNSS, and RTK-GNSS determined the linear EO parameters for each image. For IG, five ground points were distributed regularly in the overall area used as GCPs and the remaining eight points used as ICPs to check the generated photogrammetric point clouds' geometric accuracy. For DG, the known linear EO parameters are used for geo-referencing without needing GCPs, and the same eight ICPs are used. Figure 5 shows the GCP and ICP locations. For checking geometric accuracy, root mean square error (RMSE) is determined for ICPs as a difference between the static GNSS and UAV data (FGDC 1998).

$$RMSE_X = \sqrt{\frac{\sum (X_{GNSS} - X_{UAV})^2}{n}} \quad RMSE_Y = \sqrt{\frac{\sum (Y_{GNSS} - Y_{UAV})^2}{n}}$$

$$RMSE_{XY} = \sqrt{RMSE_X{}^2 + RMSE_Y{}^2} \quad RMSE_Z = \sqrt{\frac{\sum (Z_{GNSS} - Z_{UAV})^2}{n}}$$

$$RMSE_{XYZ} = \sqrt{RMSE_X{}^2 + RMSE_Y{}^2 + RMSE_Z{}^2}$$

3.1. The effect of UAV altitude AGL on UAV featureless image processing

To assess the influence of UAV flight configuration over a featureless surface for topographic applications. The impact of the UAV flight altitude AGL on both IG and DG processing was presented by studying four different heights (140, 160, 180 and 200 m) with a spatial resolution (3.41, 3.9, 4.39 and 4.68 cm/pix GSD) of 80% for both forward and lateral overlap. Figure 8 shows the scheme of UAV flight heights and

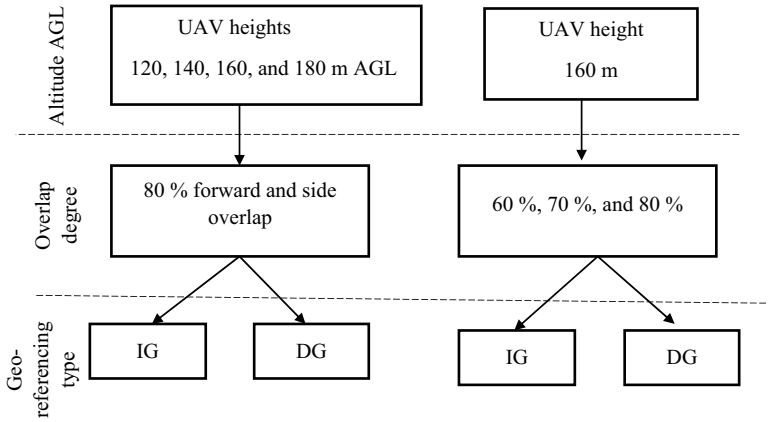

Figure 6. Scheme of UAV field configuration and processing.

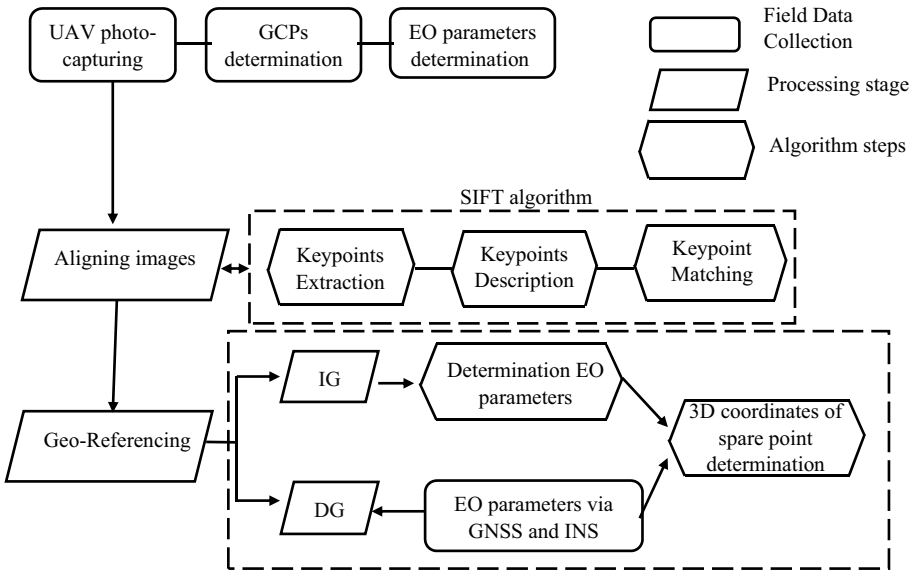

Figure 7. Flowchart of field data collection and image processing stages.

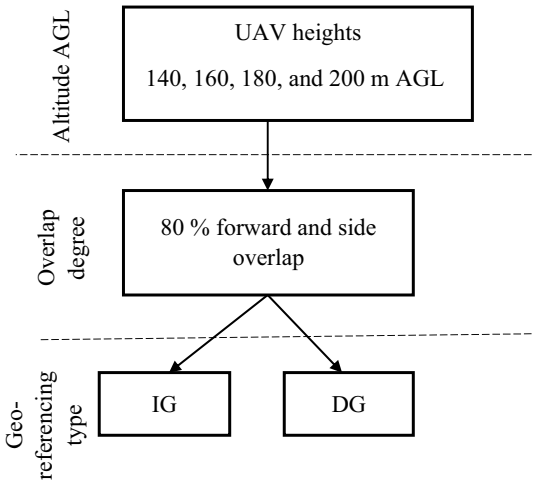

Figure 8. Scheme of UAV flight heights and processing.

processing. The flight plan consisted of strips working east–west, and the flight planning parameters of the four different altitude AGL are shown in Table 1.

3.1.1. The influence of flight altitude on IG processing of featureless UAV images

The four different altitude missions have been processed by IG processing using five GCPs and eight ICPs, as shown in Figure 5. The geometric accuracy of easting, northing and elevation is determined by calculating the RMSE of the eight ICPs from the selected flying height, shown in Table 2 and Figure 9.

Table 1 summarises the results of the geometric accuracy related to flight heights where IG process was used. It is clear from Figure 9 that the spatial accuracy is increased in northing and elevation directions whenever flying altitude is decreased. The highest geometric accuracy is obtained at the lowest flight altitude of 140 m AGL. Increasing the flight height

Table 1. The flight planning parameters of the four different altitude AGL.

Flight altitude AGL (m)	No. of flight lines	No. of photos per line	No. of total photos	Flight time (minutes)
140	49	34	1666	34.5
160	43	30	1290	27
180	38	27	1026	21.5
200	35	25	875	18.5

Table 2. The RMSE of the four different altitude AGL of IG process.

Flight height (m)	GSD (cm/pix)	Easting RMSE (m)	Northing RMSE (m)	Elevation RMSE (m)	Total RMSE (m)
140	3.41	0.023	0.015	0.033	0.043
160	3.9	0.012	0.028	0.038	0.049
180	4.39	0.017	0.03	0.039	0.052
200	4.68	0.022	0.032	0.042	0.057

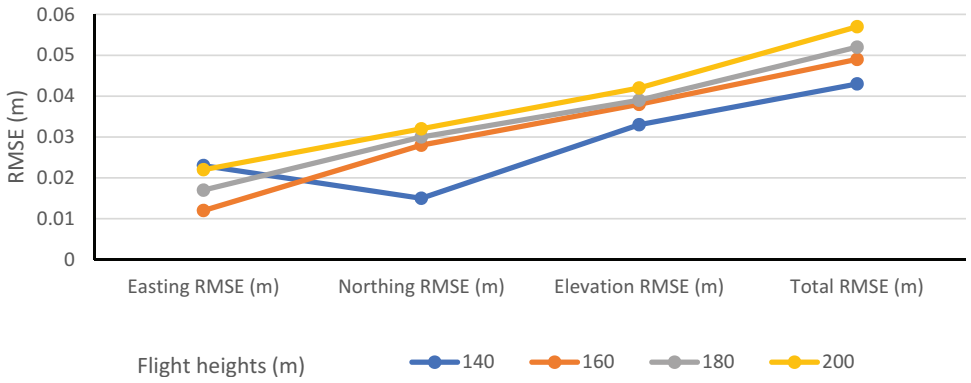

Figure 9. The correlation between the attitude AGL and RMSE of the IG process.

leads to a decrease in the achieved geometric accuracy. The highest easting accuracy was gained at 160 m height, and both northing and elevation highest geometric accuracy were produced at 140-m flight height AGL. The four different altitudes gave a close total spatial accuracy within 0.043 to 0.057 m.

Table 3 shows the common matching parameters for the four different altitudes: spare point density, correct and wrong matching point, average tie point multiplicity and matching time.

Table 3 shows that the 140 m flight height AGL gave the highest-level spare point density, correct matching points, average tie point multiplicity, matching time and lowest wrong matching points. Increasing the flight altitude leads to reduced spare point density, correct matching points, matching time and average tie point multiplicity. At the altitude of 140 m, the largest image numbers (1666) at a ground sampling distance (resolution) of 3.41 cm/pixel were acquired. The generated point cloud with approximately 227,562 3D points was extracted following the IG method. Generally, the increment of flight height can reduce flight and processing times and cost while keeping the acceptable geometric accuracy of the generated point clouds.

3.1.2. The effect of flight altitude on DG processing of featureless UAV images

The four different altitude AGL missions were processed by DG using the known linear EO parameters determined by RTK-GNSS without needing any GCPs. The eight ICPs were used for assessing the geometric accuracy of the generated point cloud. The RMSE of the eight ICPs was calculated for the three directions shown in Table 4 and Figure 10.

Table 3. The matching parameters of the four different altitude AGL of IG process.

Flight height (m)	140 m	160 m	180 m	200 m
Total points	227,562	141,767	127,254	115,342
Correct matching points	146,453	87,896	78,357	62,435
%Correct matching points	64.36%	62%	61.57%	54.13%
Wrong matching points	81,109	53,871	48,897	52,907
%Wrong matching points	35.64%	38%	38.43%	45.87%
Average tie point multiplicity	6.192	3.079	2.77	2.25
Matching time	1 day and 22 hours	1 day and 14 hours	1 day and 3 hours	20 hours and 35 minutes

Table 4. The RMSE of the four different altitude AGL of DG process.

Flight height (m)	GSD (cm/pix)	Easting RMSE (m)	Northing RMSE (m)	Elevation RMSE (m)	Total RMSE (m)
140	3.41	0.012	0.018	0.029	0.036
160	3.9	0.018	0.013	0.032	0.039
180	4.39	0.016	0.015	0.043	0.048
200	4.68	0.015	0.020	0.047	0.053

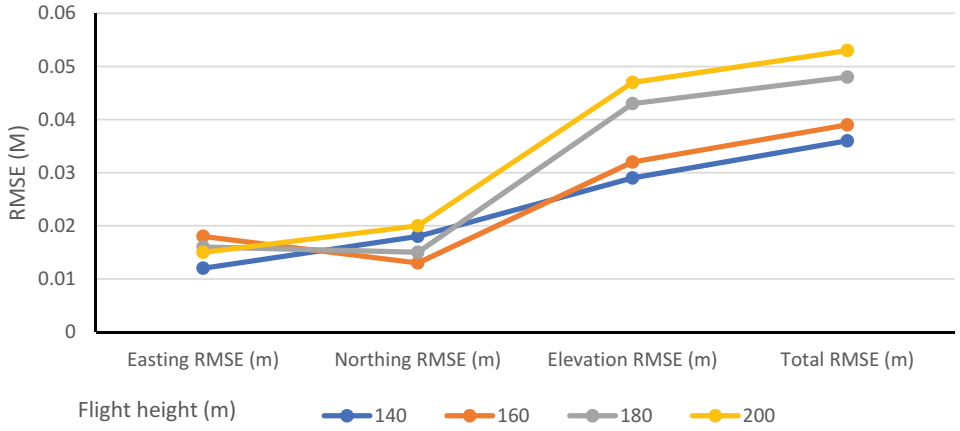

Figure 10. The correlation between the attitude AGL and RMSE of DG process.

Based on Table 4 and Figure 10, as flight height AGL is increased, RMSE of the point cloud is increased. From 140 m AGL, flight gives a geometric accuracy of 0.036 m. From 160 m AGL, the RMSE was 0.039 m. From 180 m AGL, the RMSE was 0.048 m. RMSE was 0.053 m at altitude of 200 m AGL. This result shows that when the altitude AGL increases, image GSD also increases, affecting incrementing the RMSE.

Table 5 shows the correlation between the flight height AGL and the matching parameters represented in the point density, correct & wrong matching points, average tie point multiplicity, and matching time.

As it is illustrated in Table 5, 140 m altitude AGL gives the best matching parameters except matching time. The spare point cloud, correct matching point and average tie point multiplicity are decreased by increasing altitude AGL. The highest spare point of 220,122 at 140 m with the highest correct matching points 194,629 is reduced to 78,623 spare points with 61,325 correct matching points at 200 m altitude AGL as the lowest density. Average tie point multiplicity reduced from 6.385 at 140 m AGL as the highest value to 2.63 at 200 m AGL as the lowest value. The matching time was reduced from 9 hours and 11 minutes at 140 m AGL to 5 hours and 55 minutes at 200 m AGL.

3.2. The effect of overlap degree on UAV images over non-textured surface

For assessing the influence of the forward and lateral overlap degree on processing and generating point clouds of UAV imagery over a featureless surface, three different levels of overlap degree (60%, 70% and 80%) flights are processed by the two IG and DG techniques at the same altitude 160 m AGL. The scheme of flights is shown in Figure 11. The flight plan consisted of strips working east–west, and the flight planning parameters of the three different overlap degrees are shown in Table 6.

3.2.1. Study the effect of overlap degree on IG processing of featureless UAV images

The three different overlap degree flights have been processed by IG using five GCPs and the remaining eight ground points used as ICPs. Figure 5 shows the locations of the GCPs and ICPs. The spatial accuracy assessment is determined by calculating the RMSE of the eight ICPs for easting, northing and elevation, and the results are shown in Table 7 and Figure 12.

As shown in Table 7 and Figure 12, the highest overlap degree recorded the highest spatial accuracy. Decreasing the overlap degree leads to a decrease in the spatial accuracy of the generated point clouds. 60% overlap recorded 0.685 m spatial accuracy. 70 % overlap gave 0.124 m spatial accuracy. The spatial accuracy of 0.049 m was at 80% overlap.

Besides the spatial accuracy, the matching parameters for the different overlap degree flights are calculated by the IG process. Table 8 shows the matching parameters for the three missions.

From Table 8, one can find that 80% overlap recorded the best matching parameters except matching time. The highest spare point was 141,767 points at 80% overlap with the highest correct matching point 87,896 points, which are reduced to 57,312 spare

Table 5. The matching parameters of the four different altitude AGL of DG process.

Flight height (m)	140 m	160 m	180 m	200 m
Total points	220,122	111,314	97,453	78,623
Correct matching points	194,629	96,776	84,519	61,325
%Correct matching points	88.42%	86.94%	86.73%	78%
Wrong matching points	25,493	14,538	12,934	17,298
%Wrong matching points	11.58%	13.06%	13.27%	22%
Average tie point multiplicity	6.385	3.297	2.94	2.63
Matching time	9 hours and 11 minutes	7 hours and 36 minutes	6 hours and 32 minutes	5 hours and 55 minutes

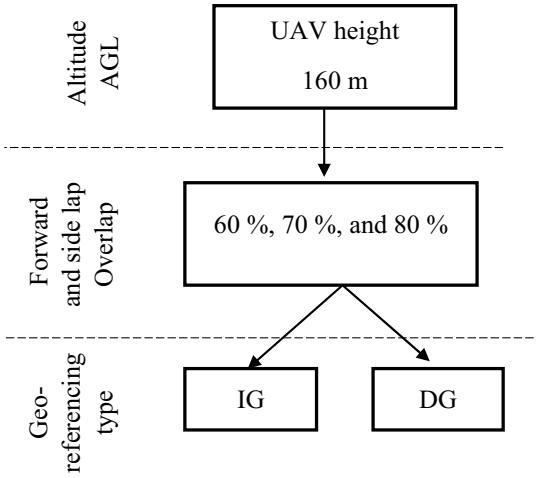

Figure 11. Scheme of UAV overlap missions and processing.

Table 6. The flight planning parameters of the four different overlap degrees.

Overlap degree (%)	No. of flight lines	No. of photos per line	No. of total photos	Flight time (min)
80	43	30	1290	27
70	29	22	638	14
60	22	17	374	8.5

Table 7. The RMSE of the three different overlap degree of IG process.

Forward and side overlap	Flight height (m)	GSD (cm/pix)	Easting RMSE (m)	Northing RMSE (m)	Elevation RMSE (m)	Total RMSE (m)
60%	160	3.9	0.11	0.225	0.638	0.685
70%	160	3.9	0.02	0.063	0.105	0.124
80%	160	3.9	0.012	0.028	0.038	0.049

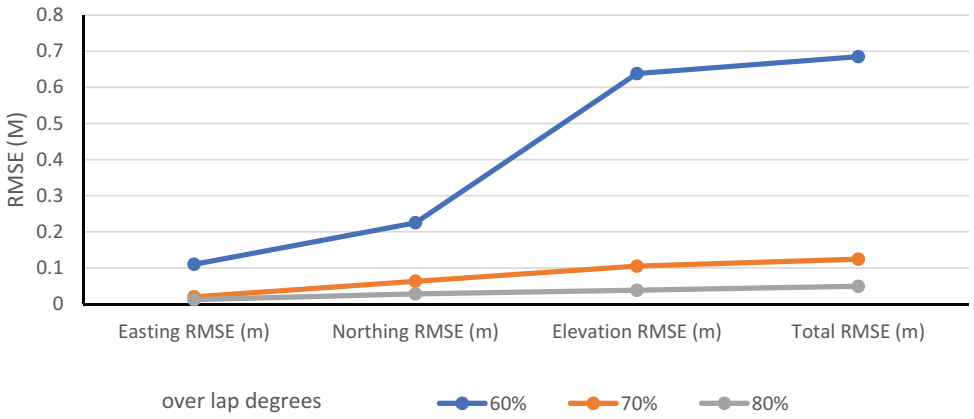

Figure 12. The correlation between the overlap degree and RMSE of IG process.

Table 8. The matching parameters of the three different overlap degrees of IG process.

Both forward and side overlap	60%	70%	80%
Total points	57,312	78,140	141,767
Correct matching points	29,413	42,516	87,896
%Correct matching points	51.32%	54.41%	62%
Wrong matching points	27,899	35,624	53,871
%Wrong matching points	48.68%	45.59%	38%
Average tie point multiplicity	2.03	2.19	3.079
Matching time	12 hours and 43 minutes	18 hours and 28 minutes	1 day and 14 hours

points with 29,413 correct matching points at 60% as the lowest density. Average tie point multiplicity reduced from 3.079 at 80% overlap as the highest value to 2.03 at 60% as the lowest value. The matching time was reduced from 1 day and 14 hours at 80% overlap to 2 hours and 43 minutes at 60% overlap.

3.2.2. The effect of overlap degree on DG processing of UAV images over the featureless surface

For assessing the effect of overlap degrees on the DG process and the spatial accuracy of photogrammetric point clouds, the three different overlap degree flights (60%, 70% and 80%) were processed using the known linear EO parameters determined by RTK-GNSS. The eight ICPs were used for assessing the geometric accuracy of the generated point cloud. The RMSE of the eight ICPs were calculated for easting, northing, elevation and total, shown in Table 9 and Figure 13.

Table 9 and Figure 13 show that 80% overlap gave the highest accuracy for the easting, northing and elevation. From 80% overlap, the mission gave a spatial accuracy of 0.039 m. From 70% overlap, the flight gave a geometric accuracy of 0.099 m. The geometric accuracy was 0.435 m with 60% overlap. Reduction overlaps to 70% might be given a suitable spatial accuracy under 0.1 m. Reduction overlaps under 70% gave an inappropriate geometric accuracy in topographic applications.

The correlation between the overlap degree and the matching parameters, the spare point density, correct and wrong matching points, average tie point multiplicity and matching time, was calculated and is shown in Table 10.

From Table 10, the 80% overlap gave the highest spare point density, highest correct matching points, highest average tie point multiplicity, high matching time and lowest wrong matching points. At the overlap of 80%, the largest image number (1290) at a ground sampling distance (resolution) of 3.9 cm/pixel was acquired. The generated point cloud with approximately 111,314 3D points was extracted following the DG method.

Generally, the increased image overlap degree leads to an increase in photogrammetric point clouds' geometric accuracy and matching parameters. The favourable results are obtained for overlap degrees at least 70% or above in the DG process.

4. The predicted geometrical accuracy formulas

This section presents new approach formulas that predict the geometrical accuracy of the generated UAV point clouds over featureless surfaces. For predicting the spatial accuracy of the UAV point clouds over featureless surfaces (which is calculated as RMSE of the checkpoints) at any value of the flight height (represented as GSD cm/pixel) and the forward and side overlap percentages, new formulas

Table 9. The RMSE of the three different overlap degrees of DG process.

Both forward and side overlap	Flight height (m)	GSD (cm/pix)	Easting RMSE (m)	Northing RMSE (m)	Elevation RMSE (m)	Total RMSE (m)
60%	160	3.9	0.208	0.159	0.348	0.435
70%	160	3.9	0.032	0.026	0.09	0.099
80%	160	3.9	0.018	0.013	0.032	0.039

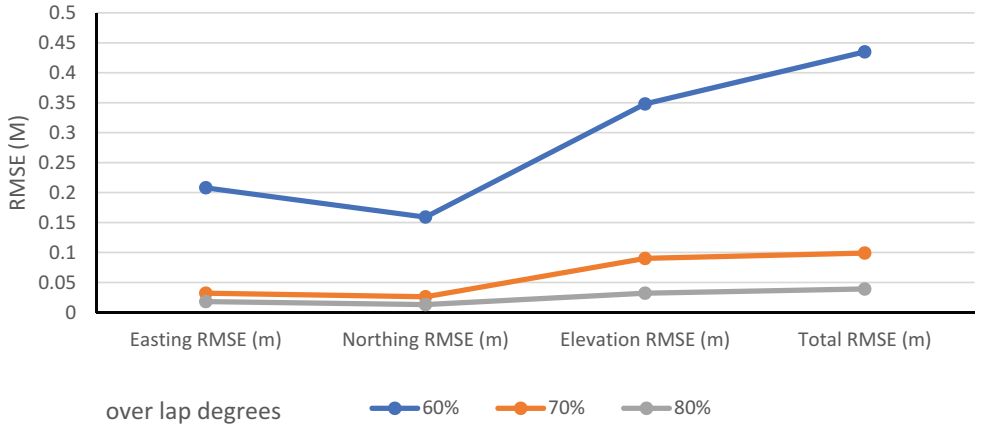

Figure 13. The correlation between the overlap degree and RMSE of DG process.

Table 10. The matching parameters of the three different overlap degrees of DG process.

Both forward and side overlap	60%	70%	80%
Total points	46,752	69,015	111,314
Correct matching points	35,877	56,220	96,776
%Correct matching points	76.74%	81.46%	86.94%
Wrong matching points	10,875	12,795	14,538
%Wrong matching points	23.26%	18.54%	13.06%
Average tie point multiplicity	2.38	2.79	3.297
Matching time	2 hour and 42 minutes	3 hours and 53 minutes	7 hours and 36 minutes

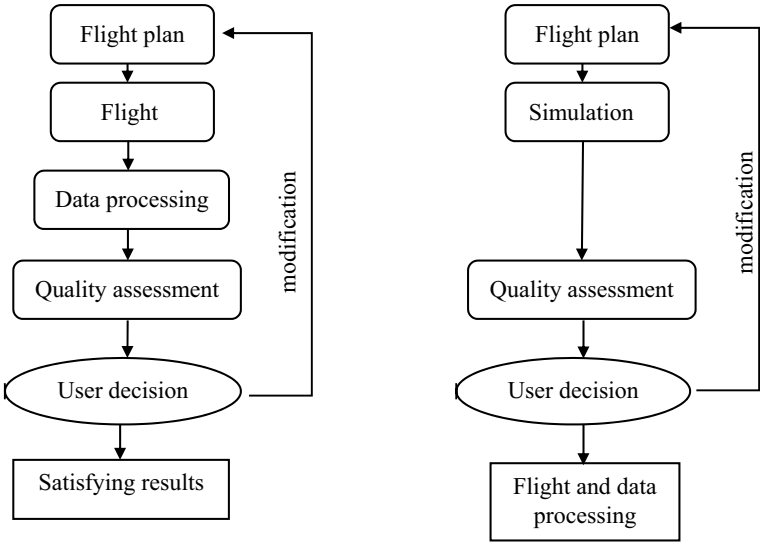

Figure 14. Conventional (left) and proposed (right) workflow from flight planning to survey.

were constructed. Both formulas gave the predicted accuracy for both types of geo-referencing (direct and indirect).

As indicated in the left part of Figure 14, the conventional loop of data acquisition, post-flight processing and derivation of the quality control at the end of the survey process is not ideal. So, we aim to construct a tool that can measure and determine the quality of the photogrammetric output measurements by simulating the acquisition process and deriving the expected quality before the flight.

Generally, we aim to shorten the loop before obtaining acceptable results regarding the conventional approach. The quality estimators are based on real data, possibly leading to repeated missions (left vs. right of Figure 14). The proposed method is based on the flight plan covering the area, with the aimed overlap ratio and flight height represented by the mean ground sampling distance. Based on these elements, the simulated flight plan is generated and the expected geometrical accuracy of the generated UAV point clouds can be derived using the new formulas. Based on this predicted geometrical accuracy, the decision to approve this flight plan or rectifying it can be taken according to the desired results. The user can interactively modify the flight plan (by selecting a different GSD or overlap) until the quality requirements are satisfied, thus maximising the probability of a successful data collection and minimising the costs. If the predicted quality is higher than the requirements, the operating procedure could be simplified, reducing the time and the cost.

According to Domingo et al. (2019), Seifert et al. (2019) and Çelik et al. (2020), geometrical accuracy is a function of image overlap, flight height, geo-referencing parameters and camera types, which can be derived in the following equation:

Geometric accuracy = f (overlap%, flight height, georeferenced parameters, camera type) + ε.

Where ε is the random error, Geo-referenced parameters are defined by GCPs for IG and EO parameters for DG and GSD cm/pixel expresses both camera type and flight height AGL. Therefore, the geometrical accuracy function can be simplified to the following formula:

Geometric accuracy = f (overlap%, GSD cm/pix, georeferencing type (DG or IG)).

4.1. Direct geo-referencing (DG) formula

The EO parameters are determined by the differential GNSS (RTK) for geo-referencing the generated point cloud. Using the results of the seven-mission shown in Tables 4 and 9, a multivariate nonlinear regression analysis using the SPSS package was used to fit the relation between geometric accuracy, image overlap and GSD cm/pixel to determine the constant coefficients that give the best fitting. This analysis produced the following relationship for the predicted geometric accuracy:

$$\text{GeometricAccuracy} = e^{\left(-10.996+\frac{609.751}{\text{overlap}}\right)} + 0.011449*\left(1.385037^{\text{GSD}}\right) - 0.0345$$

Where:

Overlap is the forward and side overlap (from 50% to 90 %).

GSD is the spatial ground sampling distance in centimetre unit (from 2 to 10 cm).

4.2. The indirect georeferencing formula

The GCPs are determined by static GNSS with a good distribution over the area (one GCP in each corner and middle). The expected geometric accuracy can be determined by using a multivariate nonlinear regression analysis using the SPSS package to fit the relation between geometric accuracy, image overlap and GSD of the seven flights shown in Tables 2 and 7:

$$\text{GeometricAccuracy} = e^{\left(-11.0624+\frac{637.608}{overlap}\right)} + 0.0154 * \left(GSD^{0.8393}\right) - 0.0454$$

Where:

Overlap is the forward and side overlap (from 50% to 90 %).

GSD is the spatial ground sampling distance in centimetres unit (from 2 to 10 cm).

These formulas are valid for a forward and side overlap between 50% and 90%, and GSD cm/pix is between 2 and 10 cm.

4.3. Formulas' precision

This section presents the formulas' precision predicting the geometrical accuracy of UAV point clouds over featureless surfaces. The proposed formulas are presented for both direct and indirect geo-referencing. These formulas are derived using seven different cases of flight height (as a GSD cm/pix) and forward and side lap over non-textured surfaces. The precision between the measured field data accuracy and predicted accuracy by the formula for the seven missions fitting these formulas is discussed.

4.3.1. DG formula

Tables 11 and 12 present the statistical characteristics for the seven mission, including the measured accuracy, prediction accuracy, formula error, maximum, average and root mean square (RMSE) errors in computing the geometrical accuracy of the UAV point cloud.

Where R^2 is the determination coefficient of the predicted formulas, which can be determined by the following expression:

$$R^2 = \left(1 - \frac{\begin{array}{c}sum\ of\ squrared\ differences\ between\\ the\ actual\ and\ predicted\ geometrical\ accuracy\ values\end{array}}{\begin{array}{c}sum\ of\ squrared\ differences\ between\ the\ actual\\ geometrical\ accuracy\ valuesandtheirmean\end{array}}\right) x100$$

$$R^2 = \left(1 - \frac{\sum^{(y-\hat{y})^2}}{\sum^{(y-\bar{y})^2}}\right) x100$$

Where:

R^2: The coefficient of determination.

y: Actual (measured) geometrical accuracy.

$\hat{y}$: The predicted geometrical accuracy.

$\bar{y}$: The mean of actual geometrical accuracy.

According to Tables 11 and 12, the absolute errors associated with the predicted formula ranged between 1.04% and 9.09%. The mean precision of the formula for the seven missions is 96.87%. The computed R^2 was 99.91 for DG formulas.

4.3.2. IG formula

The statistical characteristics for the flight missions, including the measured accuracy, prediction accuracy, formula's error, maximum, average and root mean square (RMSE) errors in computing the UAV point cloud's geometrical accuracy using IG formula are listed in Tables 13 and 14.

Tables 13 and 14 show that the absolute errors associated with the IG formula have a range between 0% and 16.13%, with an absolute mean error precision of 4.16%. The mean precision of the IG formula for the seven missions records 95.84%. The computed R^2 was 99.5 for IG formulas.

4.4. Formulas' validation

The verification dataset of five independent flight mission measurements is employed to test the accuracy of the new developed formulas. A comparison between the measured geometric accuracies of the UAV point

Table 11. The statistical characteristics for the seven missions of the DG formula.

Flight no.	GSD (cm/pix)	Forward and side overlap (%)	Measured accuracy (m)	Prediction accuracy (m)	Formula's error (m)	Formula's error (%)	Similarity (%)
Flight 1	3.41	80	0.036	0.0345	−0.0015	−4.17	95.83
Flight 2	3.9	80	0.039	0.04	0.001	2.56	97.44
Flight 3	4.39	80	0.048	0.0475	−0.0005	−1.04	98.96
Flight 4	4.68	80	0.053	0.0523	−0.0007	−1.32	98.68
Flight 5	3.9	60	0.435	0.44	0.005	1.15	98.85
Flight 6	3.9	70	0.099	0.108	0.009	9.09	90.91
Flight 7	3.9	80	0.039	0.04	0.001	2.56	97.44
Average					0.0027	3.13	96.87

Table 12. Statistics of the predicted DG formula employing the field data.

Average error	Minimum error	Maximum error	RMSE	R^2
0.0027 m 3.13%	0.0005 m 1.04%	0.009 m 9.09%	0.0015 m	99.91

Table 13. The statistical characteristics for the seven missions of the IG formula.

Flight no.	GSD (cm/pix)	Forward and side overlap (%)	Measured accuracy (m)	Prediction accuracy (m)	Formula's error (m)	Formula's error (%)	Similarity (%)
Flight 1	3.41	80	0.043	0.043	0	0	100
Flight 2	3.9	80	0.049	0.048	−0.001	−2.04	97.96
Flight 3	4.39	80	0.052	0.053	0.001	1.92	98.08
Flight 4	4.68	80	0.057	0.056	−0.001	−1.75	98.25
Flight 5	3.9	60	0.685	0.649	−0.036	−5.26	94.74
Flight 6	3.9	70	0.124	0.144	0.02	16.13	83.87
Flight 7	3.9	80	0.049	0.048	−0.001	−2.04	97.96
Average					0.0086	4.16	95.84

Table 14. Statistics of the predicted IG formula employing the field data.

Average error	Minimum error	Maximum error	RMSE	R^2
0.0086 m 4.16%	0.000 m 0%	0.036 m 16.13%	0.0059 m	99.5

cloud and those calculated by applying formulas is listed in Tables 15 and 16 and depicted in Figures 15 and 16 for IG and DG formulas.

Table 15 and Figure 15 confirmed that the tested formulas underestimate or overestimate the geometric accuracy of the UAV point cloud, with errors in the range of 9.73% and 5.39%. DG formula relationship predicted geometrical accuracy with an error of 7.27%.

Table 16 and Figure 16 showed that the predicted formula underestimate or overestimate the geometrical accuracy of the UAV point cloud, with errors in the range of 11.79% and 5.11%. Table 16 reported that the mean error in the geometric accuracy computed with the IG formula was about 8.09%.

The mean formula error % and formula error for the predicted geometrical accuracy of the derived point clouds is 7.24% and 0.00598 m for DG formula, and 8.09% and 0.006982 m for IG formula, respectively. The agreement between the computations by formulas and the independent field data is 92.76% and 91.91% for DG and IG formulas, respectively.

Table 15. The statistical validation characteristics of the DG formula.

Flight no.	GSD (cm/pix)	Forward and side overlap (%)	Measured accuracy (m)	Prediction accuracy (m)	Formula's error (m)	Formula's error (%)	Similarity (%)
Flight 1	4.39	75	0.076	0.0703	−0.0057	7.5	92.5
Flight 2	4.49	85	0.0331	0.0352	0.0021	6.34	93.66
Flight 3	3.9	65	0.221	0.205	−0.016	7.24	92.76
Flight 4	3.9	75	0.0668	0.0632	−0.0036	5.39	94.61
Flight 5	3.9	85	0.0257	0.0282	0.0025	9.73	90.27
Average					0.00598	7.24	92.76

Table 16. The statistical validation characteristics of the IG formula.

Flight no.	GSD (cm/pix)	Forward and side overlap (%)	Measured accuracy (m)	Prediction accuracy (m)	Formula's error (m)	Formula's error (%)	Similarity (%)
Flight 1	4.39	75	0.09361	0.0851	−0.00851	9.09	90.91
Flight 2	4.49	85	0.0392	0.0363	−0.0029	7.4	92.6
Flight 3	3.9	65	0.2743	0.2885	0.0142	5.18	94.82
Flight 4	3.9	75	0.086	0.08	−0.006	6.98	93.02
Flight 5	3.9	85	0.028	0.0313	0.0033	11.79	88.21
Average					0.006982	8.09	91.91

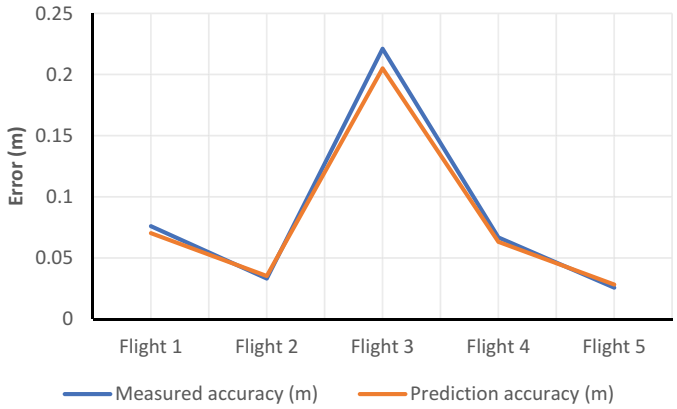

Figure 15. The comparison between the measured and prediction accuracy of the DG formula.

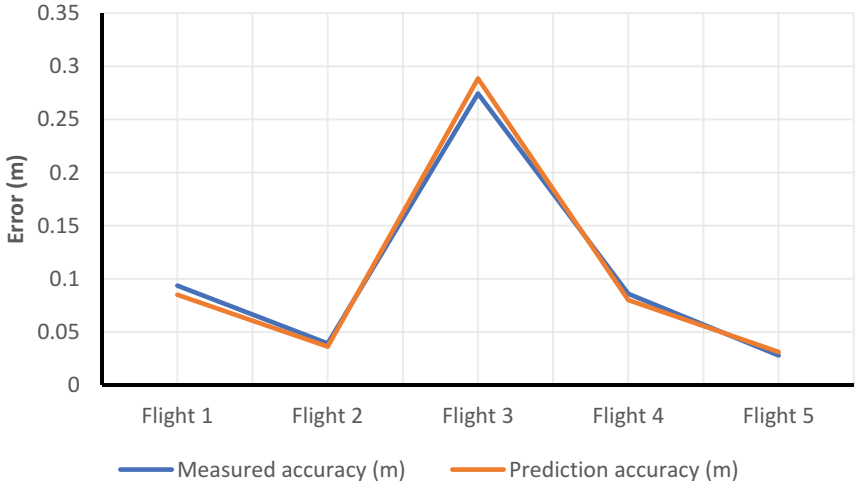

Figure 16. The comparison between the measured and prediction accuracy of the IG formula.

5. Conclusion

This article presented a practical study to use UAV images over featureless surface for topographic mapping. The paper investigates the influence of different flight heights and levels of overlap degree on the geometric accuracy of the generated topographic mapping products. The results show that the UAV photogrammetry system is useful for mapping the non-textured flat area, such as GNSS or conventional techniques. The relation between the geometric accuracy and UAV altitudes 140, 160, 180 and 200 m AGL gave 0.043, 0.049, 0.052 and 0.057 m for IG process and 0.036, 0.039, 0.048 and 0.053 m for DG process, respectively. The higher degree of overlap and low flight height recorded the highest spare point clouds, correct matching points, average tie point multiplicity, matching time and lowest wrong matching point for matching parameters.

Generally, low flight height gave high precision and the highest reconstruction. The altitude increment might reduce flight time, processing time and cost while keeping the acceptable geometric accuracy. The increasing of image overlap degree leads to an increase in photogrammetric point clouds' geometric accuracy. The favourable results are obtained for the four different altitudes and overlap degrees at least 80% or above. A multivariate nonlinear regression analysis was used to fit the relation between geometric accuracy, image overlap and GSD cm/pixel for the seven missions determining two formulas predict the geometrical accuracy of the UAV point cloud. The agreement between the computations by formulas and the independent field data is 92.76% and 91.91% for DG and IG formulas, respectively.

Disclosure statement

No potential conflict of interest was reported by the author(s).

ORCID

Ahmed Elhadary http://orcid.org/0000-0002-8111-2922

References

Aasen H, Honkavaara E, Lucieer E, Zarco-Tejada P. 2018. Quantitative remote sensing at ultra-high resolution with UAV spectroscopy: a review of sensor technology, measurement procedures, and data correction workflows. Remote Sens. 10:1091–1933. doi:10.3390/rs10071091.

Agisoft. 2019. Agisoft metashape user manual: professional Edition, Version1.6. https://www.agisoft.com/pdf/metashape-pro_1_6_en.pdf

Borgogno Mondino E, Gajetti M. 2017. Preliminary considerations about costs and potential market of remote sensing from UAV in the Italian viticulture context. Eur J Remote Sens. 50(1):310–319. doi:10.1080/22797254.2017.1328269.

Çelik M, Aydın A, Bünyan F, Kuşak L, Kanun E. 2020. The effect of different flight heights on generated digital products: DSM and Orthophoto. Mersin Photogramm J. 2 (1):01–09.

Crommelinck S, Bennett R, Gerke M, Ying Yang M, Vosselman G. 2017. Contour detection for UAV-Based cadastral mapping. Remote Sens. 9(2):171–184. doi:10.3390/rs9020171.

Daakir M, Pierrot- Deseilligny M, Bosser P, Pichard F, Thom C, Rabot Y, Martin O. 2017. Lightweight UAV with on-board photogrammetry and single-frequency GPS positioning for metrology applications. ISPRS – J Photogramm. 127:115–126. doi:10.1016/j.isprsjprs.2016.12.007.

Domingo HOØ, Næsset E, Kachamba D, Gobakken T. 2019. Effects of UAV image resolution, camera type, and image overlap on accuracy of biomass predictions in a tropical Woodland. Remote Sens. 11(8):1–17. doi:10.3390/rs11080948.

Falkner E, Morgan D. 2002. Aerial mapping: methods and applications. 2nd ed. Boca Raton (FL, USA): CRC Press.

FGDC. 1998. Geospatial positioning accuracy standards. FGDC-STD-007.3-1998, Part 3: National Standard for Spatial Data Accuracy (NSSDA).

Manfreda S, McCabe M, Miller P, Lucas R, Pajuelo Madrigal V, Mallinis G, Ben-Dor B, Helman D, Estes L, Ciraolo G. 2018. On the use of unmanned aerial systems for environmental monitoring. Remote Sens. 10(4):641–669. doi:10.3390/rs10040641.

Mesas-Carrascosa FJ, Notario García MD, Meroño de Larriva JE, García-Ferrer A. 2016. An analysis of the influence of flight parameters in the generation of Unmanned Aerial Vehicle (UAV) Orthomosaicks to Survey Archaeological Areas. Sensors (Basel, Switzerland). 16 (11):18–38. doi:10.3390/s16111838.

Rabah M, Basiouny M, Ghanem E, Elhadary A. 2018. Using RTK and VRS in direct geo-referencing of the UAV imagery. NRIAG J Astron Geophys. 7(2):220–226. doi:10.1016/j.nrjag.2018.05.003.

Seifert E, Stefan S, Holger V, David D, Jan van A, Anton K, Thomas S. 2019. Influence of drone altitude, image overlap, and optical sensor resolution on multi-view reconstruction of forest images. Remote Sens. 11(10):1252. doi:10.3390/rs11101252.